



Flow fluctuations and kinetic freeze-out of identified hadrons at energies available at the CERN Super Proton Synchrotron

Sudhir Pandurang Rode ¹, Partha Pratim Bhaduri ², and Amaresh Jaiswal³

¹*Veksler and Baldin Laboratory of High Energy Physics, Joint Institute for Nuclear Research, Dubna, 141980 Moscow region, Russian Federation*

²*Variable Energy Cyclotron Centre, HBNI, 1/AF Bidhan Nagar, Kolkata 700 064, India*

³*School of Physical Sciences, National Institute of Science Education and Research, An OCC of Homi Bhabha National Institute, Jatni-752050, Odisha, India*



(Received 20 March 2023; accepted 22 June 2023; published 11 July 2023)

We investigate the effect of flow fluctuations, incorporated in non-boost-invariant blast-wave model, on kinetic freeze-out parameters of identified hadrons in low energy relativistic heavy-ion collisions. For the purpose of this study, we use the transverse momentum spectra of the identified hadrons produced in central Pb–Pb collisions, at CERN Super Proton Synchrotron energies ranging from $E_{\text{lab}} = 20\text{A}–158\text{A}$ GeV, and analyze them within a modified non-boost-invariant blast wave model. We perform simultaneous fits of the transverse momentum spectra for light hadrons (π^- , K^\pm , p) and heavy strange hadrons (Λ , $\bar{\Lambda}$, ϕ , Ξ^\pm , Ω^\pm) separately. We also fit the transverse momentum spectra of charmonia (J/Ψ , Ψ') at $E_{\text{lab}} = 158\text{A}$ GeV. Our findings suggest that the inclusion of flow fluctuations enhances kinetic freeze-out temperature in case of light and heavy strange hadrons and reduces the corresponding transverse flow velocities. Moreover, we find that the kinetic freeze-out parameters of the charmonia at $E_{\text{lab}} = 158\text{A}$ GeV are least affected by inclusion of flow fluctuations. Based on this, we make predictions which can provide further insights on the role of flow fluctuations in relativistic heavy-ion collisions.

DOI: [10.1103/PhysRevC.108.014906](https://doi.org/10.1103/PhysRevC.108.014906)

I. INTRODUCTION

Collisions of relativistically accelerated heavy ions in the laboratory allow production and study of hot and dense quantum chromodynamics (QCD) matter [1–3]. Tuning of collision energy can enable the possibility of creating nuclear matter at various temperatures and baryon densities which can probe a large part of QCD phase diagram. The BNL Relativistic Heavy Ion Collider (RHIC) [4,5] and CERN Large Hadron Collider (LHC) [6–8] accelerate nuclei with ultrarelativistic speeds which creates medium having thermodynamic conditions of high temperatures and negligible baryon chemical potentials. Lattice QCD (lQCD) simulations [9–13] are well suited for the study of such medium.

Nuclear matter corresponding to the region of moderate temperature and finite net baryon densities in QCD phase diagram is created by lowering the beam energies. The application of lQCD to study such matter is limited. However, in recent times, the interest in studying nuclear collisions at these energies has been rejuvenated and many ongoing as well as upcoming accelerator facilities at RHIC [14], CERN

Super Proton Synchrotron (SPS) [15,16], Facility for Anti-proton Ion Research (FAIR [17,18]), and Nuclotron-based Ion Collider fAcility (NICA) [19], have performed and planned various experimental programs. This includes the beam energy scan (BES) and STAR Fxt (fixed target) program of RHIC, NA61 and NA60+ experiments at SPS, compressed baryonic matter (CBM) experiment at FAIR, and baryonic matter at the nuclotron (BM@N) and multi-purpose detector (MPD) experiment at NICA. The systematic interpretation of the available data from earlier fixed-target mode experiments at Alternating Gradient Synchrotron (AGS) and SPS facilities in these beam energy ranges can allow an appropriate utilization of the upcoming facilities. Out of several challenges, estimation of freeze-out conditions of the fireball at various beam energies has been one of the compelling topics in heavy-ion collisions.

The particle chemistry of the fireball stabilizes during the chemical freeze-out as the inelastic scatterings stop, whereas, during kinetic freeze-out, the momentum distributions of the hadrons are frozen. The quark flavor dependent multiple chemical freeze-out scenario where strange hadrons fix their composition earlier than light hadrons, was predicted by the authors of Ref. [20]. Similar observations were found for mass dependent kinetic freeze-out of the measured hadrons in the fixed target energy domain [21]. In general, the hydro-inspired blast-wave model can be used to describe kinetic freeze-out conditions [22]. The particle spectra from hydrodynamics was described by assuming the emission from cylindrically

Published by the American Physical Society under the terms of the [Creative Commons Attribution 4.0 International](https://creativecommons.org/licenses/by/4.0/) license. Further distribution of this work must maintain attribution to the author(s) and the published article's title, journal citation, and DOI. Funded by SCOAP³.

TABLE I. Summary of the fit results of p_T spectra of light and heavy strange hadrons after implementing the flow fluctuations with uniform distribution of transverse velocity, at different energies ranging from 20A to 158A GeV at SPS. The values η_{\max} are kept the same as no fluctuations scenario and adopted from Refs. [21] and [25]. The corresponding fit results in the no fluctuations scenario are quoted in parentheses.

Species	E_{lab} (A GeV)	η_{\max}	β_s^{\min}	β_s^{\max}	β_s^0	T_{kin} (MeV)	χ^2/N_{dof}	
π^-, K^\pm, p	20	1.882 ± 0.005	0.653 ± 0.002	0.852 ± 0.003	0.752 ± 0.004	(0.777 ± 0.002)	91.62 ± 0.22 (79.78 ± 0.05)	6.7 (6.5)
	30	2.084 ± 0.004	0.618 ± 0.003	0.926 ± 0.004	0.772 ± 0.005	(0.805 ± 0.002)	93.51 ± 0.23 (80.28 ± 0.05)	7.2 (6.7)
	40	2.094 ± 0.004	0.596 ± 0.003	0.873 ± 0.005	0.734 ± 0.005	(0.803 ± 0.001)	108.97 ± 0.38 (81.92 ± 0.04)	5.6 (5.5)
	80	2.391 ± 0.005	0.631 ± 0.003	0.914 ± 0.006	0.772 ± 0.007	(0.802 ± 0.002)	97.40 ± 0.40 (82.68 ± 0.05)	3.7 (3.8)
	158	2.621 ± 0.006	0.601 ± 0.004	0.925 ± 0.006	0.764 ± 0.007	(0.807 ± 0.002)	104.41 ± 0.44 (84.11 ± 0.05)	4.5 (4.4)
$\Lambda, \bar{\Lambda}, \phi, \Xi^\pm, \Omega^\pm$	20	1.288 ± 0.021	0.515 ± 0.021	0.744 ± 0.023	0.630 ± 0.016	(0.663 ± 0.005)	105.17 ± 1.53 (93.12 ± 0.19)	1.5 (1.8)
	30	1.728 ± 0.026	0.507 ± 0.021	0.772 ± 0.016	0.639 ± 0.013	(0.675 ± 0.004)	105.50 ± 1.06 (95.84 ± 0.17)	1.9 (2.2)
	40	1.752 ± 0.018	0.541 ± 0.014	0.762 ± 0.016	0.652 ± 0.011	(0.681 ± 0.004)	110.46 ± 1.17 (98.87 ± 0.13)	3.6 (3.6)
	80	1.989 ± 0.021	0.554 ± 0.008	0.722 ± 0.014	0.638 ± 0.008	(0.673 ± 0.003)	124.51 ± 1.48 (106.54 ± 0.12)	3.5 (3.4)
	158	2.031 ± 0.029	0.555 ± 0.007	0.733 ± 0.011	0.644 ± 0.006	(0.703 ± 0.002)	135.99 ± 1.24 (109.24 ± 0.11)	3.4 (3.4)

symmetric and boost-invariant fireball [23]. Over the years there have been several modifications to the original formulation of the blast wave model. Recently, the formulation of the non-boost-invariant blast-wave model [24] was employed at AGS and SPS energies in our previous works to describe the transverse and longitudinal spectra of identified hadrons [21,25].

The main assumptions in the formulation of the blast wave model are the following: the freeze-out isotherm is described at a constant proper time ($\tau = \text{const}$) and the transverse rapidity profile at the isotherm has a linear form. Other assumptions are neglecting the presence of flow fluctuations, on-mass shell distributions functions, a homogeneous number density, and the absence of resonance feed-down. The assumption of the absence of resonance feed-down has been taken into consideration by us for pions in our previous work [25]. In the present article, we have accounted for flow fluctuations following Ref. [26] which was applied to the boost-invariant blast-wave model. Due to the finite size of the systems generated in heavy-ion collisions, significant fluctuations are expected during the initial stages of the collisions. This applies even to collisions with fixed impact parameters. The initial conditions of hydrodynamical calculations are sensitive to these fluctuations whose impact can survive till the freeze-out. Therefore it is crucial to consider these fluctuations in the blast wave model. Further details regarding this implementation will be presented in the following section.

In this article, we have modified the non-boost-invariant blast-wave model following the idea from Ref. [26] and employed this modified non-boost-invariant blast-wave model to study the effect of flow fluctuations on the kinetic freeze-out conditions of identified hadrons in central Pb–Pb collisions at SPS energies. In Ref. [26], the authors have considered two different formulations, namely, flat or uniform and Gaussian distribution of hydrodynamical velocities for implementing the flow fluctuations (more details in Sec. II). To accomplish our goal, we examine the p_T spectra of identified particles within the beam energy range $E_{\text{lab}} = 20\text{A}–158\text{A}$ GeV. The identified particles are categorized according to their mass as, light hadrons (π^-, K^\pm, p) and heavy strange hadrons

($\Lambda, \bar{\Lambda}, \phi, \Xi^\pm, \Omega^\pm$) as well as charmonia (J/ψ and ψ' only at $E_{\text{lab}} = 158\text{A}$ GeV). The rapidity spectra are not analyzed in this article since it is expected to be insensitive to the changes in the transverse flow profile.¹ Our findings in this article predict higher kinetic freeze-out temperature and lower in transverse flow velocity using both uniform as well as Gaussian formulations compared to no fluctuations scenario for both light as well as heavy strange hadrons across all analyzed beam energies. Interestingly, the kinetic freeze-out temperature and transverse flow velocity corresponding to charmed hadrons do not show any significant change in both formulations with respect to the no fluctuations scenario. We also found that the mass hierarchy of the kinetic freeze-out parameters as argued in our previous analysis is still preserved even in the presence of transverse flow fluctuations.

To the best of our knowledge, this is the first attempt to incorporate the flow fluctuations into the non-boost-invariant blast-wave model to describe the transverse momentum spectra of identified hadrons at SPS energies. As mentioned earlier, authors of Ref. [26] have implemented the flow fluctuations into the boost-invariant blast-wave model to study the heavy hadrons namely, $J/\psi, \phi,$ and Ω . There was an attempt made to consider the transverse flow fluctuations in noncentral collisions by the authors of Refs. [27,28]. The authors have also used Bessel-Gaussian formulations for the descriptions of the initial state eccentricity fluctuations which are not purely Gaussian especially for peripheral collisions. Since in this article, we are exclusively dealing with central collisions, we refrain from using the Bessel Gaussian formulation.

The organization of the article is as follows. Following the Introduction in this section, the features of the blast-wave model and its modification for incorporating transverse flow fluctuations is described in Sec. II. The results are presented and discussed in Sec. III. In Sec. IV we summarize and conclude our findings from this study.

¹We have explicitly verified that the rapidity distributions are insensitive to the incorporation of fluctuations in the transverse flow profile.

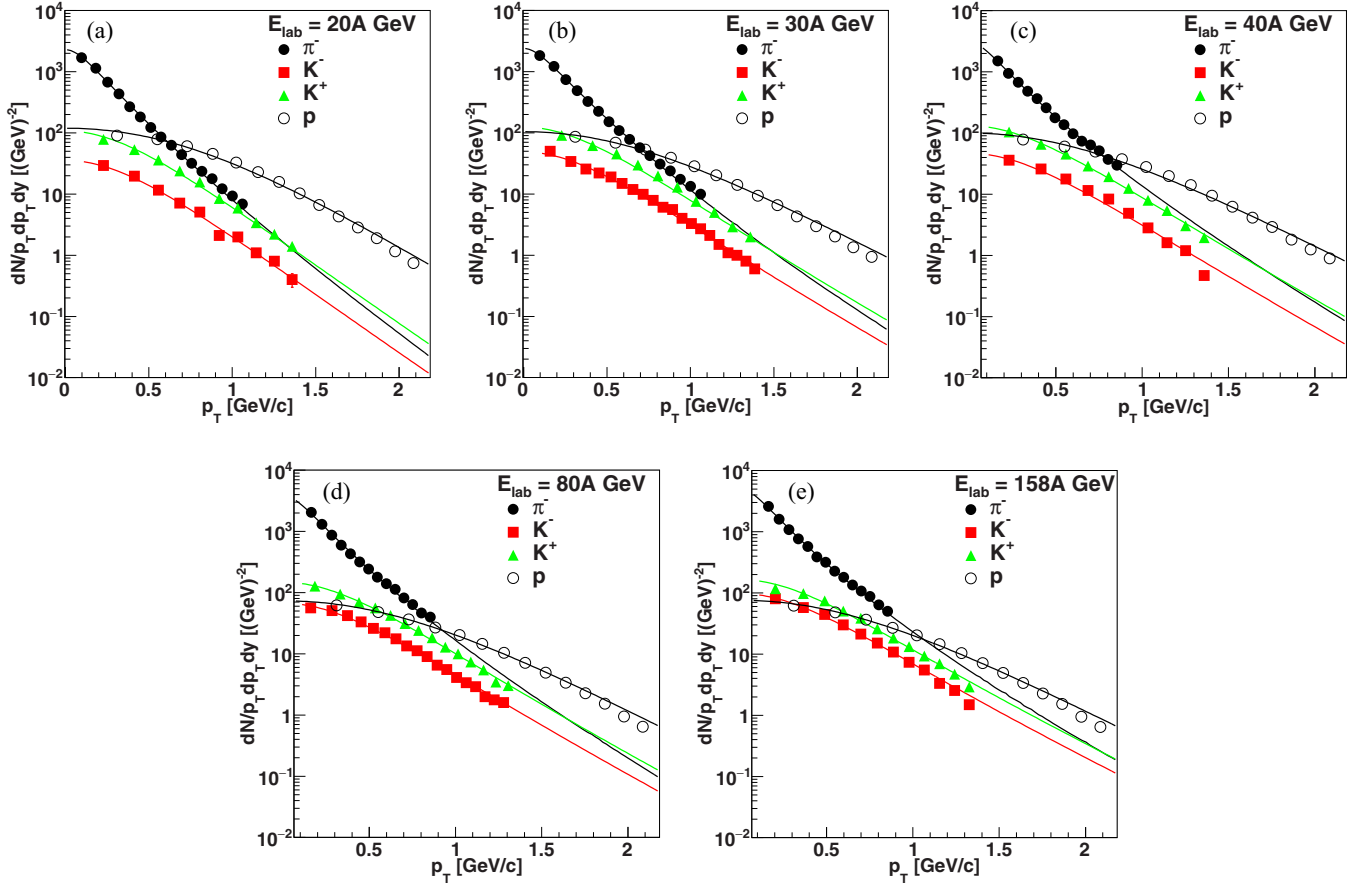


FIG. 1. Simultaneously fitted p_T spectra of π^- , K^\pm , and p at (a) 20A GeV, (b) 30A GeV, (c) 40A GeV, (d) 80A GeV, and (e) 158A GeV beam energies using uniform profile of transverse flow fluctuations. Error bars indicate available statistical error.

II. A BRIEF DESCRIPTION OF THE MODEL

In this section, we briefly introduce the non-boost-invariant blast wave model. For more details, the reader is referred to Refs. [21,24,25]. Within the framework of this model, the single particle spectrum for central collisions with respect to transverse mass $m_T (\equiv \sqrt{p_T^2 + m^2})$ and rapidity y can be written as

$$\begin{aligned} \frac{dN}{m_T dm_T dy} &= \frac{g}{2\pi} m_T \tau_F \int_{-\eta_{\max}}^{+\eta_{\max}} d\eta \cosh(y - \eta) \\ &\times \int_0^{R(\eta)} r_\perp dr_\perp I_0 \left(\frac{p_T \sinh \rho(r_\perp)}{T} \right) \\ &\times \exp \left(\frac{\mu - m_T \cosh(y - \eta) \cosh \rho(r_\perp)}{T} \right), \quad (1) \end{aligned}$$

where g is the degeneracy of particle species and η ($\equiv \tanh^{-1}(z/t)$) is the space-time rapidity. Moreover, we have $\beta_T = \tanh(\rho)$ where ρ is the flow rapidity in the transverse plane (or transverse rapidity) and β_T is the collective transverse fluid velocity. Under the assumption that the common freeze-out of the fireball is instantaneous, the freeze-out time τ_F becomes independent of the transverse coordinate r_\perp and occurs at kinetic freeze-out temperature T . Considering a Hubble like expansion of the fireball in the transverse plane,

the transverse fluid velocity has radial dependence and is assumed to have the form

$$\beta_T(r_\perp) = \beta_s \left(\frac{r_\perp}{R(\eta)} \right), \quad (2)$$

where β_s denotes the transverse fluid velocity at the surface of the fireball. It is important to note that in the above equation, we have $R(\eta)$ in the denominator as opposed to R_0 in the model from Ref. [24]. Due to this characteristic, for a given nonzero η , the transverse flow goes to zero at the center and takes the maximum value β_s at the edges of the fireball as r_\perp approaches to $R(\eta)$. For the case of a linear parametrization, the average transverse flow velocity becomes $\langle \beta_T \rangle = \frac{2}{3} \beta_s$ and thus it is independent of η .

As discussed earlier, it is important to note that the presence of flow fluctuations has been neglected in the differential spectra shown in Eq. (1). Because of the finite system size, large fluctuations in the initial stage of the heavy-ion collisions may appear, even in the central collisions. These fluctuations can affect the initial conditions of the hydrodynamical expansion of the medium. Moreover, owing to the nonlinear nature of hydrodynamic equations, the event average of any hydrodynamical parameter is quite different from that for a smooth initial configuration. This leads to large differences in spectra obtained from hydrodynamical

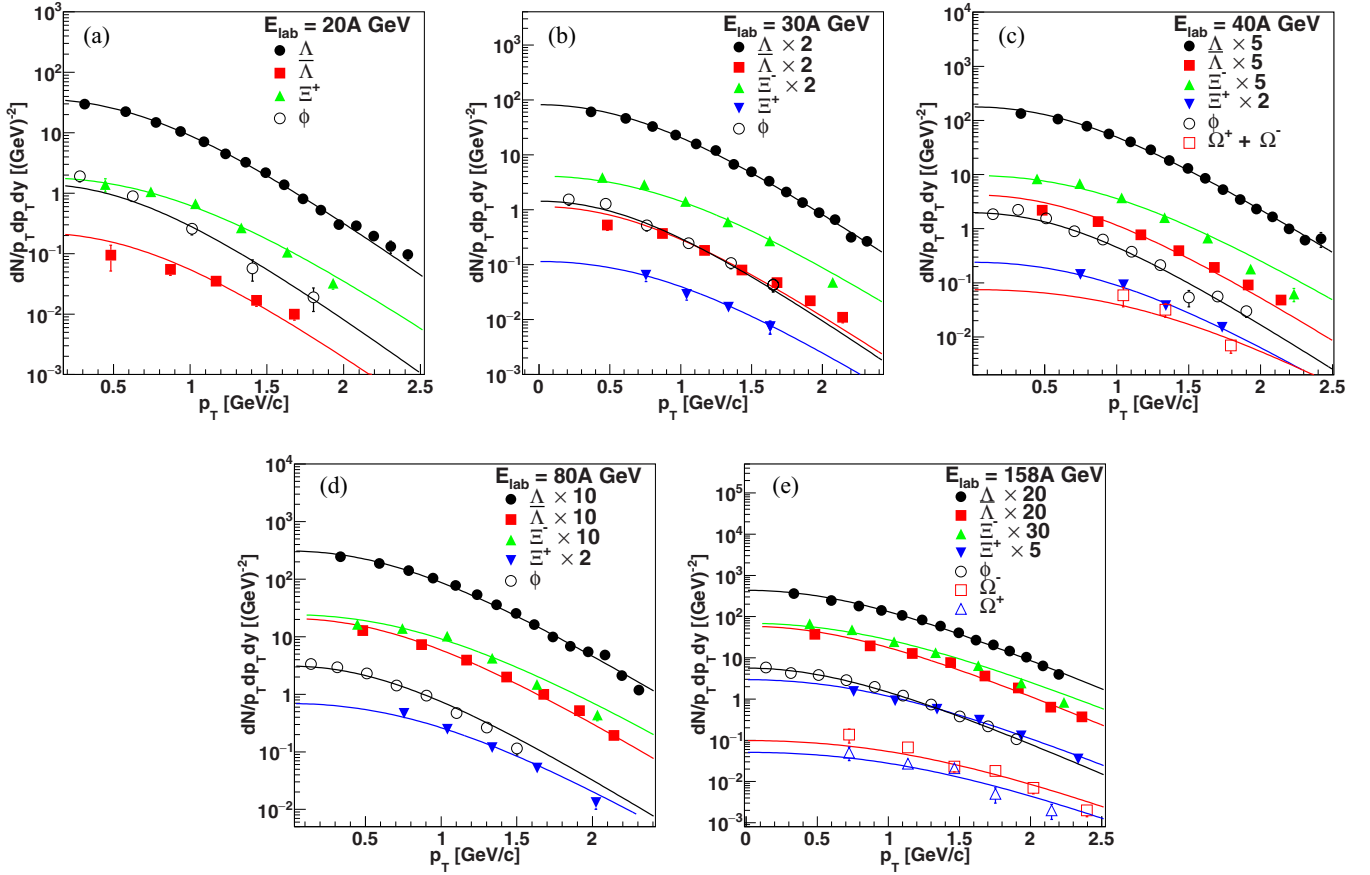


FIG. 2. Simultaneously fitted p_T spectra of Λ , $\bar{\Lambda}$, ϕ , Ξ^\pm , and Ω^\pm at (a) 20A GeV, (b) 30A GeV, (c) 40A GeV, (d) 80A GeV, and (e) 158A GeV beam energies using uniform profile of transverse flow fluctuations. Error bars indicate available statistical error.

calculations with averaged initial conditions, compared to fluctuating initial conditions [29–31]. Therefore it is important to incorporate the collective flow fluctuations in blast-wave model to examine their effect on the kinetic-freeze-out parameters. To this end, we consider new form of a non-boost-invariant blast-wave model averaged over an ensemble of the fluctuations, motivated from Ref. [26] for the transverse surface velocity, β_s as

$$\begin{aligned} \frac{dN}{m_T dm_T dy} &\propto \frac{g}{2\pi} m_T \tau_F \int_{\beta_s^{\min}}^{\beta_s^{\max}} d\beta_s F(\beta_s) \\ &\times \int_{-\eta_{\max}}^{+\eta_{\max}} d\eta \cosh(y - \eta) \\ &\times \int_0^{R(\eta)} r_\perp dr_\perp I_0 \left[\frac{p_T \sinh \rho(r_\perp)}{T} \right] \\ &\times \exp \left[\frac{\mu - m_T \cosh(y - \eta) \cosh \rho(r_\perp)}{T} \right]. \end{aligned} \quad (3)$$

We consider two different profiles for distribution of β_s ,

$$F(\beta_s) = \begin{cases} 1 & : \text{Uniform} \\ \exp \left[-\frac{(\beta_s - \beta_s^0)^2}{\delta^2} \right] & : \text{Gaussian} \end{cases}. \quad (4)$$

In the first case, a flat or uniform distribution of hydrodynamical velocities is considered with β_s^{\min} and β_s^{\max} being

the lower and upper limit of the transverse flow velocities. The average of uniform distribution is defined as $\beta_s^0 = (\beta_s^{\min} + \beta_s^{\max})/2$. In the second case, a Gaussian distribution of hydrodynamical velocities is assumed with β_s^0 and δ being the mean and standard deviations, respectively. In this case, the lower and upper limit of the transverse flow velocities are taken to be 0 and 1, respectively.

To make up for limited available incident energy, the freeze-out volume is restricted in the region $-\eta_{\max} \leq \eta \leq \eta_{\max}$, assuming the reflection symmetry about the center of mass. The transverse size is parametrized considering the elliptic shape of fireball in reaction plane, as follows:

$$R(\eta) = R_0 \sqrt{1 - \frac{\eta^2}{\eta_{\max}^2}}, \quad (5)$$

where R_0 denotes the transverse size of the fireball at $\eta = 0$. The dependence on R_0 factors out after changing the integral variable $r_\perp \rightarrow r_\perp/R$ in Eq. (3) which lead to an overall factor of volume, $\tau_F R_0^2$. Moreover, the assumption of the boost-invariance is relaxed by the explicit dependence of system boundary in the transverse plane on the longitudinal coordinate, as parametrized in Eq. (5). At the freeze-out surface, the temperature is assumed to be constant. Moreover, the transverse flow gradient is independent of r_\perp and it has only η dependence through $R(\eta)$. One can notice from Eq. (3) that

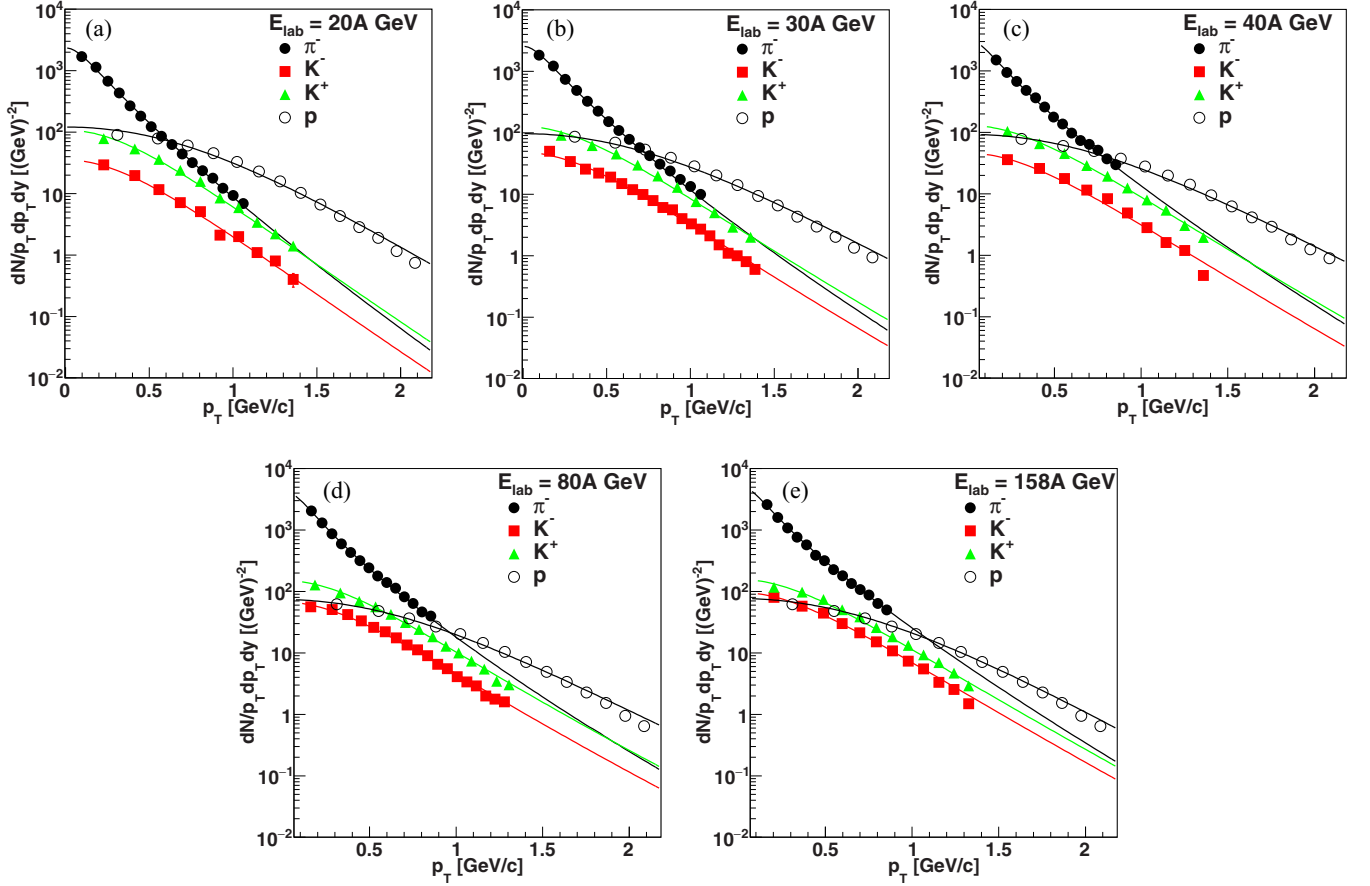


FIG. 3. Simultaneously fitted p_T spectra of π^- , K^\pm , and p at (a) 20A GeV, (b) 30A GeV, (c) 40A GeV, (d) 80A GeV, and (e) 158A GeV beam energies using a Gaussian description of transverse flow fluctuations. Error bars indicate available statistical error.

the variable r_\perp takes values between $0 \leq r_\perp \leq R(\eta)$. However, the transverse velocity $\beta_T(r_\perp)$ given in Eq. (2) remains finite and lies in the physical range (preserves causality) for $\beta_s < 1$, even though $R(\eta) \rightarrow 0$ as $\eta \rightarrow \pm\eta_{\max}$. In addition, we observe from Eq. (2) that the transverse flow gradient along r_\perp diverges as $\eta \rightarrow \pm\eta_{\max}$. This makes the model unsuitable for those analyses involving the quantities which depend on gradients, such as dissipative effects. Nevertheless, in our framework we do not deal with such gradients since we are employing the nondissipative blast wave model and hence such issues are not encountered in the implementation of this model.

One may argue that because of the elliptic shape of the fireball in the reaction plane in Eq. (5), the system size decreases away from midrapidity and hence flow fluctuations may get stronger. Therefore, the parameters in Eq. (4) should depend on space-time rapidity. However, it is important to note that almost all of the analyzed species in the present work are measured at midrapidity. Moreover, the η dependence of temperature was studied in Ref. [24]. The authors concluded that the change in the temperature due to this dependence is small without compromising the χ^2/NDF , which suggests that the same might also be true for transverse velocity. Therefore the effect of η dependence on the model parameters is expected to be small and hence is ignored in the present work.

III. RESULTS AND DISCUSSIONS

Results obtained from this study have been presented and discussed in this section. For this purpose, we have analyzed the measured transverse momentum spectra (p_T) of light, heavy strange, and charmed (only at $E_{\text{lab}} = 158\text{A GeV}$) hadrons produced in central Pb–Pb collisions from NA49 and NA50 collaborations [32–34] at SPS in the beam energy range $E_{\text{lab}} = 20\text{A}–158\text{A GeV}$. The hadrons analyzed in this paper were categorized according to their masses, following the intuition that heavy particles may decouple earlier than lighter ones. Note that we have focused only at SPS energies as the data for heavier particles in the desired kinematic regions are barely available at lower beam energies. Resonance decay contributions to the lightest hadron in our dataset, i.e., pions, are taken into consideration following the formalism in Ref. [35]. All p_T spectra analyzed here are calculated at the center of the measured rapidity region (e.g., at $y_{\text{c.m.}} = 0.1$, for $0 < y_{\text{c.m.}} < 0.2$) of the hadron. We have explicitly checked that fit of p_T spectra at the central value of measured rapidity coverage of a particular species do not yield any significant changes in the values of the parameters when compared with the parameters obtained by fitting the spectra integrated over the measured rapidity region. Therefore, the main message of our paper remains unaltered. The fits of p_T spectra are performed simultaneously for each category of hadrons by

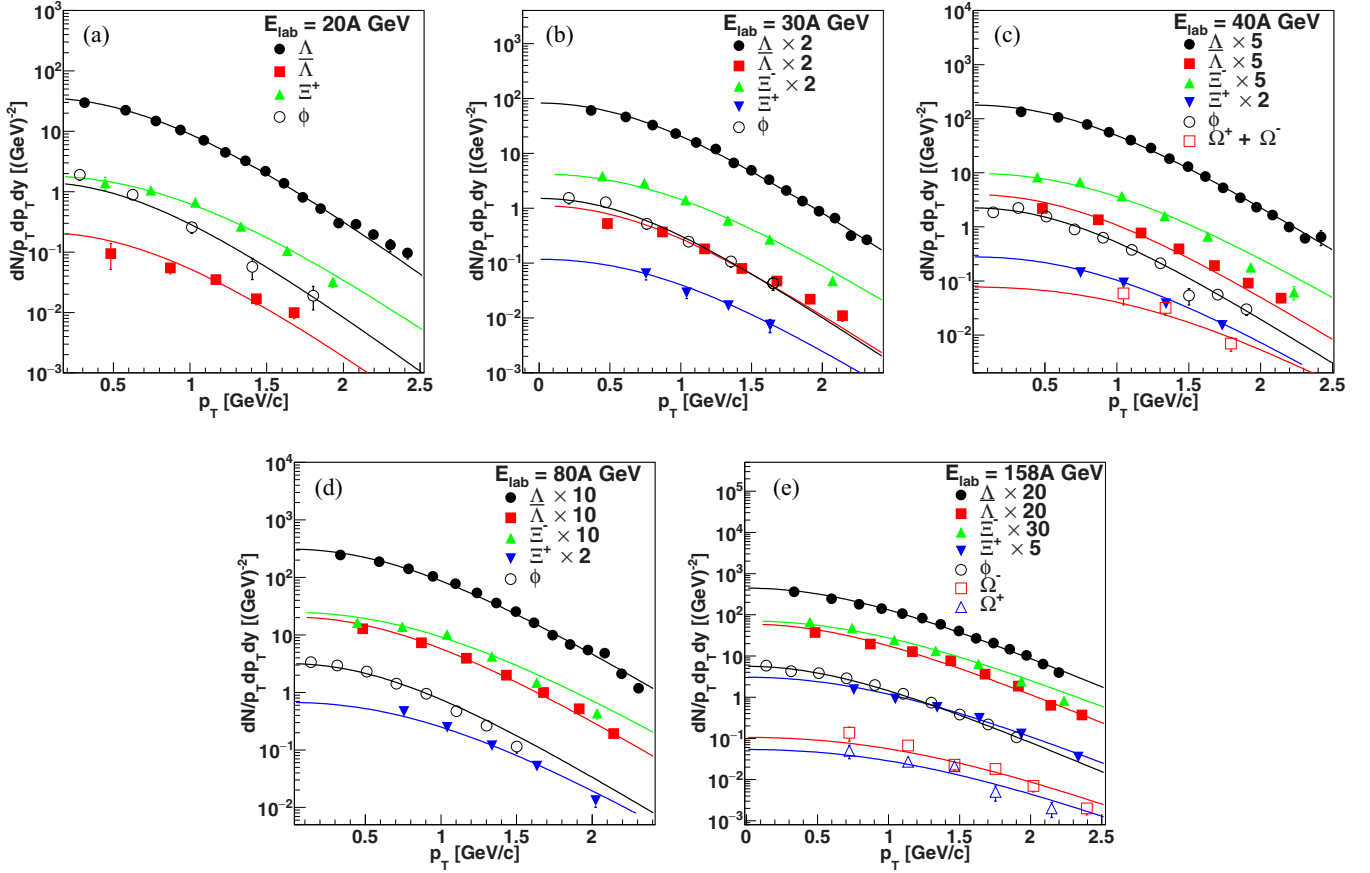


FIG. 4. Simultaneously fitted p_T spectra of Λ , $\bar{\Lambda}$, ϕ , Ξ^\pm , and Ω^\pm at (a) 20A GeV, (b) 30A GeV, (c) 40A GeV, (d) 80A GeV, and (e) 158A GeV beam energies using a Gaussian description of transverse flow fluctuations. Error bars indicate available statistical error.

minimizing the value of χ^2/N_{dof} , where N_{dof} is the number of degrees of freedom defined as the number of data points minus the number of fitting parameters. In our analysis, the minimization procedure was performed using the MINUIT [36] package available in ROOT framework [37].

For the adopted linear transverse flow profile, essentially, there are three parameters associated with our non-boost-invariant blast-wave model; see Eq. (1). These parameters are T_{kin} , η_{max} , and β_s out of which two parameters, T_{kin} and β_s are sensitive to the p_T spectra. On the other hand, the p_T spectra are rather insensitive to η_{max} and the rapidity spectra are insensitive to the other two parameters, T_{kin} and β_s . Moreover, because of the non-Bjorken flow, the rapidity spectra are sensitive to η_{max} [25,38]. This was the main reason that we did not consider analyzing rapidity spectra of the hadrons under study using Eq. (3). Along with this, we also checked this explicitly by fitting the rapidity spectra by integrating Eq. (3) with respect to p_T to obtain the desired longitudinal spectra and we found that the parameter, η_{max} is unchanged. Therefore, we have used the values of η_{max} obtained from our previous analyses [21,25], where, the values of η_{max} , T_{kin} , and β_s were obtained recursively. First, η_{max} is fixed from the simultaneous fits of the rapidity distributions with initial guess of T_{kin} and β_s , and then this η_{max} is used to fit corresponding p_T distributions. These newly extracted T_{kin} and β_s values are

then used to get updated η_{max} . This procedure converges rather quickly.

As discussed in Sec. II, there are two cases, namely, uniform and Gaussian distributions, corresponding to the form of fluctuations $F(\beta_s)$, considered in this study. First, we start by fitting the p_T spectra of light and heavy strange hadrons using Eq. (3) with the former case, $F(\beta_s) = 1$. Using this approach we extract three parameters, namely, β_s^{min} , β_s^{max} , and T_{kin} . For the comparison, the average of the uniform distribution is also estimated which is defined as $\beta_s^0 = (\beta_s^{\text{min}} + \beta_s^{\text{max}})/2$. The quality of the fits is better than and in few cases similar to the default case, i.e., no fluctuations scenario.

The obtained fit parameters are tabulated in Table I and corresponding fit to the spectra is shown in Figs. 1 and 2. We have noticed that the predicted new T_{kin} values are higher than the ones from our previous analyses, where it was between 80–85 MeV for light hadrons and 90–110 MeV for heavy strange hadrons. This seems to be the consequence of the implementation of the flow fluctuations into our model, to which the initial hydrodynamical conditions are expected to be sensitive and subsequently, affect the kinetic–freeze-out conditions. It is important note that for a uniform flow fluctuation profile, the fitted value of transverse flow velocity is smaller than the default case, i.e., without fluctuations. In order to compensate for smaller transverse flow velocity, the

TABLE II. Summary of the fit results of p_T spectra of light and heavy strange hadrons after implementing the flow fluctuations with Gaussian distribution of transverse velocity, at different energies ranging from 20A to 158A GeV at SPS. The values η_{\max} are kept the same as the no fluctuations scenario and adopted from Refs. [21] and [25]. The corresponding fit results in the no fluctuations scenario are quoted in parentheses.

Species	E_{lab} (A GeV)	η_{\max}	β_s^0	δ	T_{kin} (MeV)	χ^2/N_{dof}
π^-, K^\pm, p	20	1.882 ± 0.005	0.736 ± 0.002 (0.777 \pm 0.002)	0.085 ± 0.001	93.58 ± 0.17 (79.78 \pm 0.05)	7.2 (6.5)
	30	2.084 ± 0.004	0.767 ± 0.002 (0.805 \pm 0.002)	0.109 ± 0.002	94.02 ± 0.19 (80.28 \pm 0.05)	6.6 (6.7)
	40	2.094 ± 0.004	0.744 ± 0.002 (0.803 \pm 0.001)	0.095 ± 0.002	102.69 ± 0.28 (81.92 \pm 0.04)	4.9 (5.5)
	80	2.391 ± 0.005	0.747 ± 0.003 (0.802 \pm 0.002)	0.127 ± 0.003	102.47 ± 0.35 (82.68 \pm 0.05)	3.1 (3.8)
	158	2.621 ± 0.006	0.738 ± 0.003 (0.807 \pm 0.002)	0.084 ± 0.002	109.23 ± 0.38 (84.11 \pm 0.05)	3.7 (4.4)
$\Lambda, \bar{\Lambda}, \phi, \Xi^\pm, \Omega^\pm$	20	1.288 ± 0.021	0.582 ± 0.009 (0.663 \pm 0.005)	0.035 ± 0.008	115.51 ± 2.72 (93.12 \pm 0.19)	1.4 (1.8)
	30	1.728 ± 0.026	0.603 ± 0.006 (0.675 \pm 0.004)	0.101 ± 0.013	108.22 ± 1.09 (95.84 \pm 0.17)	2.0 (2.2)
	40	1.752 ± 0.018	0.615 ± 0.004 (0.681 \pm 0.004)	0.079 ± 0.011	115.02 ± 1.30 (98.87 \pm 0.13)	3.6 (3.6)
	80	1.989 ± 0.021	0.602 ± 0.005 (0.673 \pm 0.003)	0.058 ± 0.008	129.87 ± 1.68 (106.54 \pm 0.12)	3.6 (3.4)
	158	2.031 ± 0.029	0.610 ± 0.003 (0.703 \pm 0.002)	0.083 ± 0.007	137.80 ± 1.16 (109.24 \pm 0.11)	3.6 (3.4)

fitted value of the kinetic freeze-out temperature is larger than the default case. This may be attributed to the fact that both transverse flow velocity and temperature leads to hardening of transverse momentum spectra

Moving on to the second case of flow fluctuations, we have used the Gaussian description of hydrodynamical ve-

locities [Eq. (4)] and have fitted the p_T spectra of light and heavy strange hadrons using Eq. (3) as shown in Figs. 3 and 4, respectively. In this case, we have fixed the lower and upper limits of the Gaussian function, $F(\beta_s)$ to be 0 and 1, respectively. However, the parameters T_{kin} , δ , and β_s^0 are kept as free. Here, as well, the quality of the fits is better,

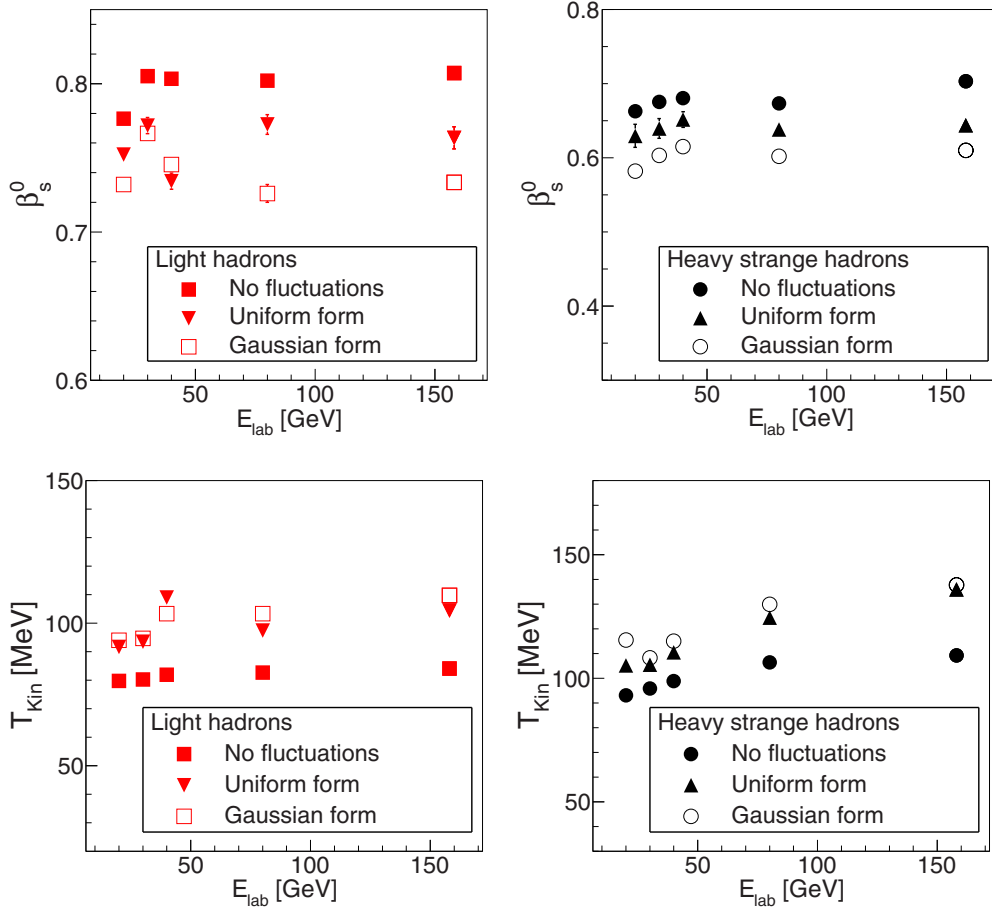


FIG. 5. Variation of the β_s^0 (top two plots) and T_{kin} (bottom two plots) for heavy strange and light hadrons with incident beam energy (E_{lab}). β_s^0 estimated for the case of uniform fluctuations is obtained by taking the mean of β_s^{\min} and β_s^{\max} . Visible vertical bars are associated errors on the parameters and for the rest of the parameters, errors are within the marker size.

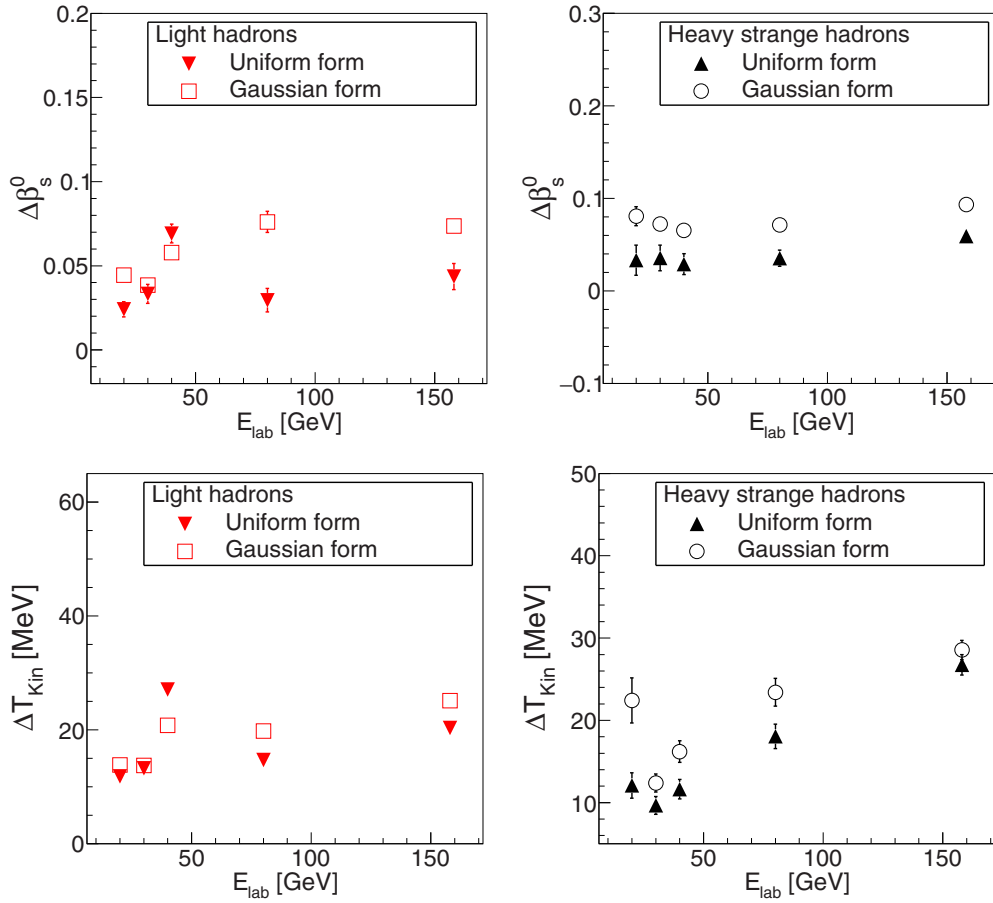


FIG. 6. Difference of T_{kin} ($\Delta T_{\text{kin}} = |T_{\text{kin}}^{\text{UF/GF}} - T_{\text{kin}}^{\text{NF}}|$) and β_s^0 ($\Delta\beta_s^0 = |\beta_s^{\text{NF}} - \beta_s^{\text{UF/GF}}|$) of light and heavy strange hadrons for both uniform and Gaussian forms with respect to the no fluctuations scenario as a function of beam energy. Vertical bars are propagated errors after the subtraction.

and in a few cases similar to the no fluctuations scenario. The fit parameters obtained from this analysis are tabulated in Table II. The observation is that the T_{kin} values are even higher than the uniform description case and β_s^0 values are smaller than the ones from our previous analyses, where it was between 0.77–0.82 for light hadrons and 0.65–0.70 for heavy strange hadrons. Moreover, values of δ parameter vary between 0.03–0.15 for both light hadrons and heavy strange hadrons.

As mentioned earlier, in the case of the Gaussian flow fluctuation profile the transverse flow velocity is even smaller than uniform flow fluctuation profile. Therefore, in order to compensate for smaller transverse flow velocity, the fitted value of kinetic freeze-out temperature is larger than the uniform case. One may argue that because of the fixed limits on the Gaussian distribution, i.e., 0 and 1, the tails may cut asymmetrically and subsequently, the central point of the Gaussian distribution may not be correct parameter, instead, the average β_s may be better parameter to compare with uniform profile scenario. However, we have checked that the average and the central values agree up to three decimal places, and therefore, it makes no significant difference to the results.

Next we look at the beam energy dependence of these extracted fit parameters as shown in Fig. 5. Here, we have

compared the values of β_s^0 and T_{kin} of light hadrons and heavy strange hadrons obtained from this study with no fluctuations scenario. Now, variation in the values of these parameters can be clearly seen in case of flow fluctuation with respect to no fluctuations. It is also interesting to observe even stronger beam energy dependence of T_{kin} in the case of the flow fluctuations. Moreover, looking at the excitation functions of these parameters qualitatively, one may find the trends interesting. To investigate this in detail, we estimate the differences of T_{kin} and β_s^0 with respect to the no fluctuations case, $\Delta T_{\text{kin}} = |T_{\text{kin}}^{\text{UF/GF}} - T_{\text{kin}}^{\text{NF}}|$ and $\Delta\beta_s^0 = |\beta_s^{\text{NF}} - \beta_s^{\text{UF/GF}}|$ as a function of beam energies as shown in Fig. 6. These quantities have a nonmonotonous structure for both uniform as well as Gaussian formulations, with a minima/maxima around $E_{\text{lab}} \approx 30\text{A}–40\text{A}$ GeV which is an interesting beam energy region. There has been many instances in the beam energy domain, $E_{\text{lab}} = 20\text{A}–158\text{A}$ GeV where various observables have shown some interesting irregularities around $E_{\text{lab}} \approx 30\text{A}–40\text{A}$ GeV [39]. This behavior has often been linked to the potential signature of the onset of deconfinement. However, in our case, one needs to be careful and perform more detailed investigations to make any robust claims.

Moving on, charmonia, i.e., J/ψ , ψ' have been analyzed in the boost-invariant scenario [40] and in the

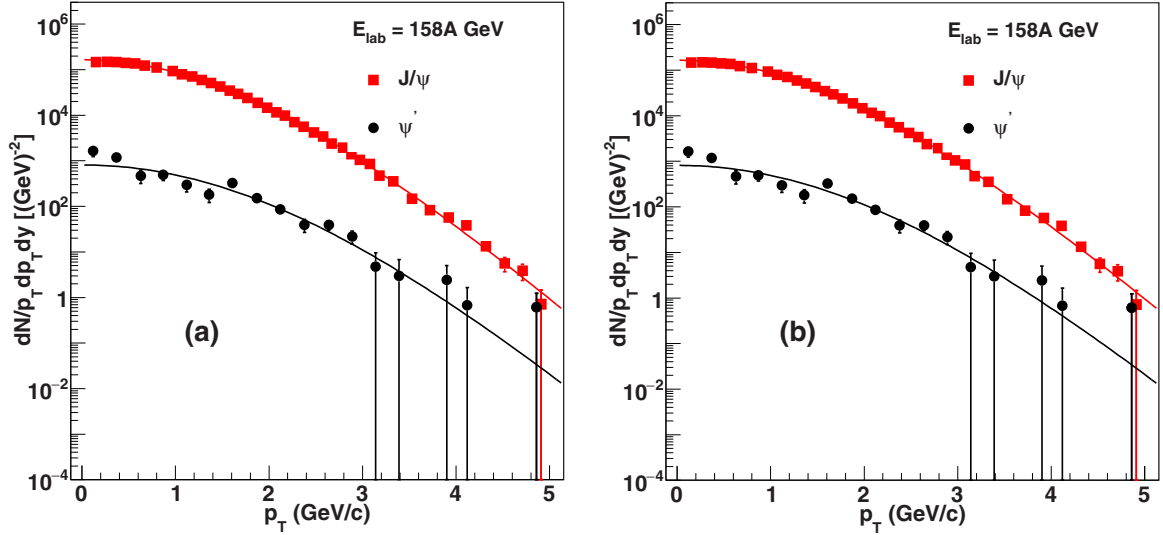


FIG. 7. Simultaneously fitted p_T spectra of J/ψ and ψ' at 158A GeV beam energies using (a) uniform and (b) Gaussian description of transverse flow fluctuations. Error bars indicate available statistical error.

non-boost-invariant case as well [21], based on the hypothesis that the production of these hadrons happened through statistical coalescence and further freeze-out during hadronization. In the present study, after light and heavy strange hadrons, a similar exercise was performed for J/ψ and ψ' [41] at $E_{\text{lab}} = 158A$ GeV. Note that same η_{max} value ($= 1.70$) from our previous study was used for the fits. Similar fit quality as our previous analysis has been achieved here as well for both uniform and Gaussian distribution of the transverse velocities. The values of the parameters in the uniform distribution

case are $\beta_s^{\text{min}} = 0.24$, $\beta_s^{\text{max}} = 0.36$, and $T_{\text{kin}} = 164$ MeV. For Gaussian flow fluctuations we obtain $T_{\text{kin}} = 165$ MeV, $\delta = 0.05$, and $\beta_s^0 = 0.3$. The corresponding fit to the spectra is shown in Fig. 7. Interestingly enough, the values of both T_{kin} and β_s^0 are found to be similar to the case of no fluctuations, which was, $T_{\text{kin}} = 164$ MeV and $\beta_s^0 = 0.3$. Moreover, the β_s^0 and its spread are lower than those of light and heavy strange hadrons where the freeze-out parameters, T_{kin} and β_s^0 , showed sensitivity to the assumption of flow fluctuations.

In Fig. 8, an updated partial expansion history of the fireball after incorporation of the flow fluctuations into the transverse momentum spectra is presented. The freeze-out parameters for light, heavy strange, and charmed hadrons obtained with no fluctuations and Gaussian prescription are plotted at $E_{\text{lab}} = 158A$ GeV. It is very interesting to see that the effect of flow fluctuations on the freeze-out parameters for charmed hadrons is quite small compared to other two groups of species. This can be interpreted as follows: Due to small rescattering cross sections in the hadronic phase, the momentum distributions of charmonia are also frozen near the phase boundary, similar to their chemical composition closer to the hadronization. This reflects in the fact that T_{kin} for charmonia is close to T_c or T_{CFO} . Because of this, the radial flow and associated fluctuations are not fully developed and show insensitivity as opposed to heavy strange and light hadrons. Our study may provoke more efforts in this direction as well as subsequent studies from us will be performed in due time.

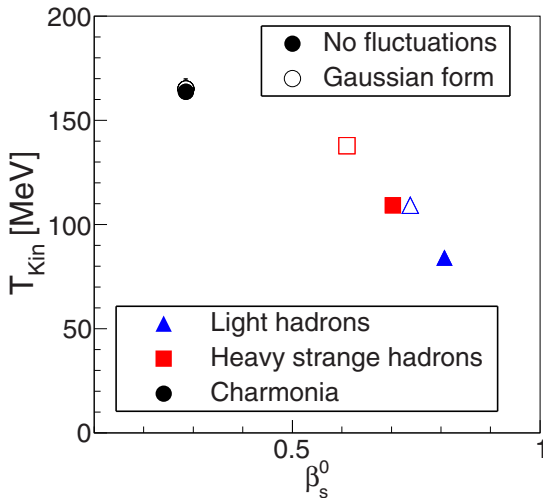


FIG. 8. The (partial) expansion history of the fireball created in 158A GeV central Pb–Pb collisions. The points indicate the temperature (T_{kin}) and transverse collective flow velocity (β_s^0) of the system at the time of light hadron kinetic freeze-out (filled triangle), heavy strange kinetic freeze-out (filled square), and charm kinetic freeze-out (filled circle). The values corresponding to Gaussian form of fluctuations are shown in empty symbols. Errors on the parameters are within the marker size.

IV. SUMMARY

To summarize, we have made some efforts to study the effect of flow fluctuations on the kinetic freeze-out parameters of various particle species. For this purpose, we have modified the non-boost-invariant blast-wave model following Ref. [26] where the authors incorporated the flow fluctuations into the boost-invariant blast-wave model. Two different functional

forms of the β_s distribution were considered, namely uniform and Gaussian descriptions. We analyzed the transverse momentum spectra of different hadron species in central Pb–Pb collisions at different SPS beam energies. The transverse momentum spectra were fitted simultaneously to obtain various freeze-out parameters such as β_s^0 and T_{kin} . The temperatures obtained using both descriptions showed higher values compared to the case of the no fluctuations scenario where it was between 80–85 MeV for light hadrons and 90–110 MeV for heavy strange hadrons. With the inclusion of flow fluctuations, the temperature varies between 90–110 MeV for light hadrons and 105–140 MeV for heavy strange hadrons. Similarly, a decrease in the β_s^0 values was observed for both descriptions at all beam energies with respect to the no fluctuations scenario where it was between 0.77–0.82 for light hadrons and 0.65–0.70 for heavy strange hadrons. Incorporation of fluctuations made β_s to reduce between 0.73–0.76 for light hadrons and 0.58–0.64 for heavy strange hadrons. Moreover, we saw a stronger increase in the temperature as a function of beam energies compared to the no fluctuations scenario. Furthermore, values of standard deviation, i.e., δ parameter varies between 0.03–0.15 for both light hadrons and heavy strange hadrons. We also fitted the charmonia at $E_{\text{lab}} = 158A$ GeV and found that the temperature as well as β_s^0 values remain almost unchanged for both descriptions with respect to the no fluctua-

tions scenario. This suggests that the incorporation of flow fluctuations does not affect the kinetic freeze-out conditions for charmonia. This could be due to the fact that the radial flow and corresponding fluctuations are not fully developed due to the freezing of momentum spectra immediately after or simultaneously at chemical freeze-out and therefore, the parameters are robust against the flow fluctuations. This is one of the interesting findings of our work.

As an outlook, these results can trigger further attempts to look at the flow fluctuations more closely at different centralities and also in the explanation of anisotropic flow coefficients. When the experimental measurements of anisotropic flow coefficients of identified hadrons including charmonia with various cumulants becomes available, the findings of this model can be verified. Moreover, it will be interesting to repeat such an exercise with charmed hadrons for lower energy collisions, when the data become available. This can be achieved with the upcoming measurements at SPS and we leave this analysis for the future.

ACKNOWLEDGMENT

A.J. is supported in part by the DST-INSPIRE faculty award under Grant No. DST/INSPIRE/04/2017/000038.

-
- [1] W. Florkowski, *Acta Phys. Pol. B* **45**, 2329 (2014).
 - [2] U. W. Heinz, [arXiv:hep-ph/0407360](https://arxiv.org/abs/hep-ph/0407360).
 - [3] P. Braun-Munzinger and J. Wambach, *Rev. Mod. Phys.* **81**, 1031 (2009).
 - [4] J. Adams *et al.* (STAR Collaboration), *Nucl. Phys. A* **757**, 102 (2005).
 - [5] K. Adcox *et al.* (PHENIX Collaboration), *Nucl. Phys. A* **757**, 184 (2005).
 - [6] K. Aamodt *et al.* (ALICE Collaboration), *Phys. Rev. Lett.* **107**, 032301 (2011).
 - [7] G. Aad *et al.* (ATLAS Collaboration), *Phys. Rev. C* **86**, 014907 (2012).
 - [8] S. Chatrchyan *et al.* (CMS Collaboration), *Phys. Rev. C* **89**, 044906 (2014).
 - [9] Z. Fodor and S. D. Katz, [arXiv:0908.3341](https://arxiv.org/abs/0908.3341).
 - [10] A. Bazavov *et al.*, *Phys. Rev. D* **80**, 014504 (2009).
 - [11] S. Borsanyi, G. Endrodi, Z. Fodor, A. Jakovac, S. D. Katz, S. Krieg, C. Ratti, and K. K. Szabo, *J. High Energy Phys.* **11** (2010) 077.
 - [12] A. Bazavov *et al.* (HotQCD Collaboration), *Phys. Rev. D* **90**, 094503 (2014).
 - [13] S. Borsanyi, Z. Fodor, C. Hoelbling, S. D. Katz, S. Krieg, and K. K. Szabo, *Phys. Lett. B* **730**, 99 (2014).
 - [14] A. Bzdak, S. Esumi, V. Koch, J. Liao, M. Stephanov, and N. Xu, *Phys. Rep.* **853**, 1 (2020).
 - [15] M. P. Lewicki *et al.* (NA61/SHINE Collaboration), [arXiv:2002.00631](https://arxiv.org/abs/2002.00631).
 - [16] M. Agnello *et al.* (NA60+ Collaboration), [arXiv:1812.07948](https://arxiv.org/abs/1812.07948).
 - [17] T. Ablyazimov *et al.* (CBM Collaboration), *Eur. Phys. J. A* **53**, 60 (2017).
 - [18] P. Senger (CBM Collaboration), *Particles* **2**, 499 (2019).
 - [19] N. S. Gerakiev (NICA/MPD Collaboration), *J. Phys.: Conf. Ser.* **1390**, 012121 (2019).
 - [20] S. Chatterjee, R. M. Godbole, and S. Gupta, *Phys. Lett. B* **727**, 554 (2013).
 - [21] S. P. Rode, P. P. Bhaduri, A. Jaiswal, and A. Roy, *Phys. Rev. C* **102**, 054912 (2020).
 - [22] W. Florkowski and W. Broniowski, *Acta Phys. Pol. B* **35**, 2895 (2004); W. Florkowski, *Nucl. Phys. A* **774**, 179 (2006).
 - [23] E. Schnedermann, J. Sollfrank, and U. Heinz, *Phys. Rev. C* **48**, 2462 (1993).
 - [24] H. Dobler, J. Sollfrank, and U. W. Heinz, *Phys. Lett. B* **457**, 353 (1999).
 - [25] S. P. Rode, P. P. Bhaduri, A. Jaiswal, and A. Roy, *Phys. Rev. C* **98**, 024907 (2018).
 - [26] S. V. Akkelin, P. Braun-Munzinger, and Y. M. Sinyukov, *Phys. Rev. C* **81**, 034912 (2010).
 - [27] S. A. Voloshin, A. M. Poskanzer, and R. Snellings, *Landolt-Bornstein* **23**, 293 (2010).
 - [28] J. Y. Ollitrault, A. M. Poskanzer, and S. A. Voloshin, *Phys. Rev. C* **80**, 014904 (2009).
 - [29] Y. Hama, T. Kodama, and O. Socolowski, Jr., *Braz. J. Phys.* **35**, 24 (2005).
 - [30] R. P. G. Andrade, F. Grassi, Y. Hama, T. Kodama, and W. L. Qian, *Phys. Rev. Lett.* **101**, 112301 (2008).
 - [31] Y. Hama, R. P. G. Andrade, F. Grassi, W. L. Qian, and T. Kodama, *Acta Phys. Pol. B* **40**, 931 (2009).
 - [32] C. Alt *et al.* (NA49 Collaboration), *Phys. Rev. C* **78**, 034918 (2008).
 - [33] C. Alt *et al.* (NA49 Collaboration), *Phys. Rev. Lett.* **94**, 192301 (2005).

- [34] C. Alt *et al.* (NA49 Collaboration), *Phys. Rev. C* **78**, 044907 (2008).
- [35] J. Sollfrank, P. Koch, and U. W. Heniz, *Phys. Lett. B* **252**, 256 (1990); *Z. Phys. C* **52**, 593 (1991).
- [36] F. James and M. Roos, *Comput. Phys. Commun.* **10**, 343 (1975).
- [37] V.5.34/32, CERN ROOT, 2015, <http://root.cern.ch>.
- [38] L. Du, H. Gao, S. Jeon, and C. Gale, [arXiv:2302.13852](https://arxiv.org/abs/2302.13852).
- [39] M. Bleicher, *J. Phys. G* **38**, 124035 (2011).
- [40] M. I. Gorenstein, K. A. Bugaev, and M. Gazdzicki, *Phys. Rev. Lett.* **88**, 132301 (2002).
- [41] M. C. Abreu *et al.* (NA50 Collaboration), *Phys. Lett. B* **499**, 85 (2001).